Three-Dimensional Finite Element Simulation of the Seismic Behavior of Multitier Concentrically Braced Frames

C. D. Stoakes[1] and L. A. Fahnestock[2]

[1]Department of Civil and Environmental Engineering, The University of Iowa, 4105 Seamans Center for the Engineering Arts and Sciences, 103 South Capitol St, Iowa City, IA 52242; email: christopher-stoakes@uiowa.edu
[2]Department of Civil and Environmental Engineering, University of Illinois at Urbana-Champaign, 2108 Newmark Civil Engineering Laboratory, 205 North Mathews Ave, Urbana, IL 61801; email: fhnstck@illinois.edu

ABSTRACT

Multitier concentrically braced frames (MTCBFs) are often employed as the lateral force-resisting system in structures where a tall, single story is required. To create an MTCBF, a braced frame is subdivided into a series of tiers with intermediate struts. Out-of-plane bracing is not provided at the tier levels, however. Prior studies on the seismic behavior of MTCBFs demonstrated that frames designed according to contemporary seismic provisions are susceptible to inelastic drift concentration within a single tier. Concentration of inelastic drift may lead to brace fracture and in-plane flexural yielding of the columns. In this study, three-dimensional finite element models of full MTCBFs were used to investigate their seismic behavior. Results from static pushover and nonlinear response history analyses revealed that the gusset plate connections at the tier levels aid MTCBFs in preventing inelastic drift concentrations and flexural yielding in the columns. Nevertheless, refinements to existing seismic design provisions appear necessary since excessive panel drifts were observed.

INTRODUCTION

Multitier concentrically braced frames (MTCBFs) are often employed as the lateral force resisting system in building and non-building structures where a tall, single story is required. To create an MTCBF, a braced frame is subdivided into multiple tiers with intermediate struts in the plane of the frame. Out-of-plane bracing is not provided at the tier levels, however. Dividing the frame into tiers reduces the effective length of the braces and the in-plane effective length of the columns. The out-of-plane effective length of the columns remains equal to the height of the braced frame. Typically, a wide flange shape with weak axis oriented in the plane of the frame is used for the braced frame columns since the out-of-plane effective length is significantly larger than the in-plane effective length. One example of a two-tier CBF is shown in Figure 1.

Prior studies on the seismic behavior of MTCBFs demonstrated that frames designed according to contemporary seismic provisions are susceptible to inelastic

drift concentration within a single tier (Imanpour et al. 2012a, 2012b, 2013; Imanpour and Tremblay 2012). Concentration of inelastic drift within a single tier may result in brace fracture due to ultra low cycle fatigue (Roufegarinejad and Tremblay 2012, Fell et al. 2009), or weak-axis flexural yielding of the columns (Imanpour et al. 2012a, 2012b, 2013; Imanpour and Tremblay 2012; Stoakes and Fahnestock 2012b). In addition to compromising in-plane stability of the columns, previous research found that weak-axis flexural yielding may also lead to out-of-plane and/or torsional column instability (Imanpour et al. 2012b; Stoakes and Fahnestock 2012b). Clearly, refinements to existing design provisions are needed to insure adequate seismic response of MTCBFs.

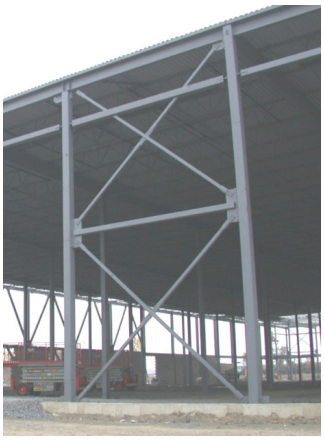

Figure 1. Two-tier concentrically braced frame (Imanpour and Tremblay 2012).

In addition, existing studies on the seismic behavior of MTCBFs have not fully accounted for column axial forces, or torsional loading and deformation of the columns in MTCBFs. In the studies by Imanpour et al. (2012a, 2012b, 2013) and Imanpour and Tremblay (2012), torsion-induced shear stresses acting on the columns were not considered to interact with normal stresses due to axial and flexural demands. In the study by Stoakes and Fahnestock (2012b), the axial force was assumed uniform over the height of the columns. The studies listed above also neglected the torsional moment and deformation induced in the wide flange columns due to out-of-plane brace buckling.

Thus, the purpose of the present study was to investigate the seismic stability behavior of MTCBFs using three-dimensional finite element models of full MTCBFs. By modeling entire frames, realistic axial loading due to ground acceleration is generated in the columns, and torsional deformation of the columns due to out-of-plane brace buckling may be simulated. In addition, the in-plane flexural restraint provided to the columns by the gusset plate connections at each tier level is included in the finite element models. The ability of connections with gusset plates to enhance the lateral response of braced frames has been well documented in existing literature (Stoakes and Fahnestock 2011, Thornton 1991, Gross and Cheok 1988, Richard 1986). Both static pushover (SPO) and nonlinear response history (NLRH) analyses were used to simulate the seismic response of MTCBFs in this study. The results from the SPO and NLRH analyses will be used to formulate design provisions for MTCBFs that ensure frame stability and prevent brace fracture.

FRAME GEOMETRY AND DESIGN

To study the seismic behavior of MTCBFs, three frames of varying heights were designed and detailed according to the American Institute of Steel Construction (AISC) *Seismic Provisions for Structural Steel Buildings* (AISC 2010b). The frames were originally designed and detailed as part of the study conducted by Imanpour et al. (2013). The prototype building containing the frames was a single-story industrial facility, located in coastal California, with a rectangular footprint of 128.8 m x 50.4 m. The lateral force-resisting system consisted of two MTCBFs per exterior wall, each with a width of 5.6 m. Frames with heights of 9 m and 2 tiers, 15 m and 3 tiers, and 24 m and 4 tiers were investigated. Single-tier X-bracing was selected as the bracing configuration and all tiers were assumed to be equal height. The design roof dead load was D = 1.2 kPa, and the design roof live load was L_r = 0.96 kPa (ASCE 2010). In addition, the exterior wall cladding was assumed to weigh 1.2 kPa, which was included in the seismic weight calculations.

Seismic forces for the design of the MTCBFs were found using the equivalent lateral force procedure, including forces due to accidental torsion. The mapped spectral response accelerations were S_s = 1.5g for short periods and S_1 = 0.6g for a 1 sec period (ASCE 2010). The structure was assigned to Seismic Design Category (SDC) D based on the mapped spectral accelerations in conjunction with the assumption that the structure was located on a class D site. In addition, the structure was assigned an earthquake importance factor of I_e = 1.0 based on the building conforming to the requirements for Risk Category II structures (ASCE 2010). Finally, the Special Concentrically Braced Frame (SCBF) seismic force-resisting system was chosen for the MTCBFs.

Once the member forces were calculated, the member sizes were selected based on the AISC *Specification for Structural Steel Buildings* (2010c). ASTM A992 wide flange shapes were used for the columns and struts, and the braces were ASTM A500, Gr. C., hollow structural sections (HSS). Since Imanpour et al. (2013) focused on the seismic behavior of the 24 m MTCBF, this frame was selected for detailed three-dimensional finite element study. This frame had W24x131 columns, W10x39 struts, and HSS4x4x5/16 braces. Since an earlier study by Stoakes and Fahnestock (2012b) indicated that torsional restraint at the tier levels has a significant impact on the buckling strength of wide flange columns in MTCBFs, the struts were oriented with their webs in the horizontal plane. With their webs oriented horizontally, the struts satisfied the minimum stiffness and strength requirements for torsional braces formulated by Helwig and Yura (1999). For brevity, the frame examined will be designated the 'scbf-24m-4tier' frame. For additional details on the design of the MTCBFs, the paper by Imanpour et al. (2013) should be consulted.

FINITE ELEMENT MODEL

Computational models of the MTCBFs were created using Abaqus FEA (2011) software. The finite element mesh for the scbf-24m-4tier model is shown in Figure 2a, and a close-up of the strut-column-brace connection is shown in Figure 2b. Four-node shell elements, with reduced integration of the element stiffness matrix,

were used to model the columns, braces, gusset plates, and splice plates. A 500-mm long strut stub was also modeled with shell elements within the strut-column-brace connection region at each tier level. Gauss quadrature with three integration points was used for the thickness integration when forming the element stiffness matrices. Figure 2b also shows that the mesh discretization was finer in the connection regions to capture stress concentrations in these areas.

Outside the tier-level connection region, the struts were modeled with three-dimensional beam elements with cubic shape functions. The leaning column, as well as the rigid link connecting the leaning column to the MTCBF, were also modeled with three-dimensional beam elements. Beam elements were used to reduce computational expense by decreasing the number of degrees-of-freedom in the MTCBF models.

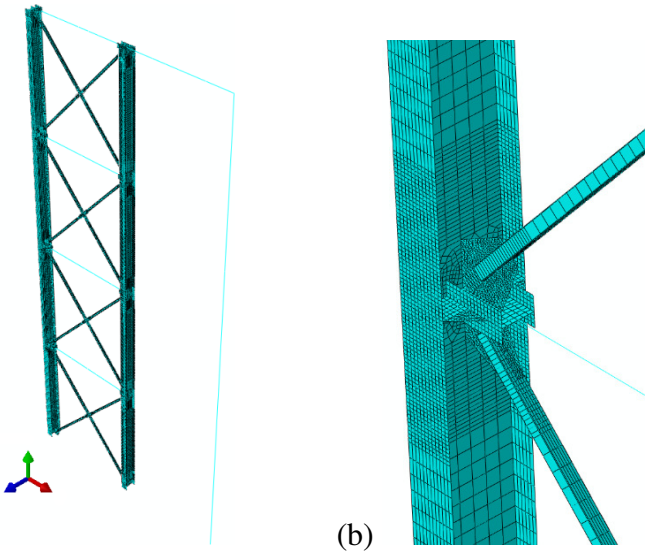

(a) (b)

Figure 2. MTCBF finite element model: (a) full frame; (b) strut-column-brace connection.

Geometric nonlinearity was incorporated in the computational models through large-displacement element formulations. Material nonlinearity was incorporated through the Maxwell-Huber-Hencky-von Mises yield criterion with associated flow rule. At the bottom of the MTCBF columns and leaning column, the three translational degrees of freedom and rotation about the *y*-axis (torsion) were restrained to simulate pinned column bases. At the top of all the columns, only the out-of-plane (*z*-direction) translation was restrained. Gravity loads, based on the load combination 1.05D + 0.25L (FEMA 2009), were applied as concentrated forces at the top of all three columns.

To account for variations in the material properties of the braces and construction quality of the brace connections, the yield stress in Panel 1 was assumed to be 5% lower than the yield stress in the remaining panels. This procedure was also used in the study by Imanpour et al. (2013). Panel 1 was selected to have weak braces since the column axial forces are largest in the bottom tier of an MTCBF, which indicates that inelastic drift concentration in Panel 1 may cause column instability at smaller roof drift ratios than drift concentration in other panels.

Static Pushover Analysis Models. For the SPO analyses, nonlinear material behavior was taken from prior experimental studies. For the ASTM A992 steel in the columns and struts, the material behavior was taken from uniaxial tension test data reported by Stoakes and Fahnestock (2012a). For the ASTM A572, Gr. 50, steel used for the gusset and splice plates, the material behavior was taken from uniaxial tension tests performed by Kauffman and Pense (1999). And, for the ASTM A500, Gr. C, steel used for the HSS braces, the material behavior was taken from uniaxial tension tests conducted by Peng (2001). The Cauchy stress vs. logarithmic strain data for each constitutive model used in the SPO analyses is illustrated in Figure 3. Isotropic strain hardening was assumed for all materials in the SPO analyses.

Since the seismic weight of an MTCBF is primarily concentrated at the roof level, an SPO load of 1 kN was applied at the top of the MTCBFs (ASCE 2010). The SPO load was divided equally between the columns in the braced frames. The Riks arc-length technique was used to increment the nodal forces and displacements, which allowed the post-ultimate strength behavior of the frames to be quantified. The Newton-Raphson method was used to solve the nonlinear field equations (Abaqus FEA 2011).

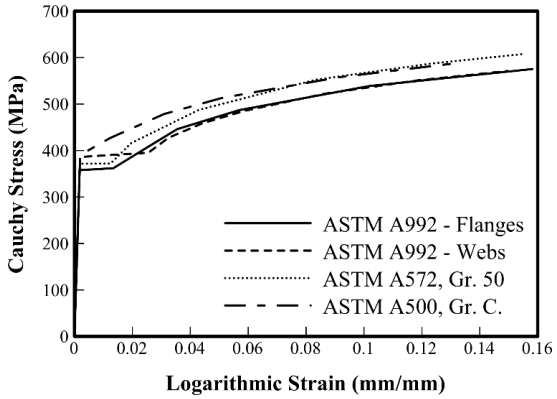

Figure 3. Cauchy stress (ksi) vs. logarithmic strain for steel materials.

Nonlinear Response History Analysis Models. For the NLRH analyses, ground acceleration time history was prescribed for the in-plane direction (*x*-direction) at the base of the left-hand column in the MTCBFs. Acceleration at the bases of the right hand MTCBF column and the leaning column were constrained to the acceleration of the left-hand MTCBF column using constraint equations (Abaqus FEA 2011). The 22 record, far-field ground acceleration suite contained within FEMA P695 (2009) was used as the basis for the NLRH analyses. The ground acceleration time histories were normalized by peak ground velocity and then scaled so the median spectral acceleration of the ground acceleration suite matched the code-prescribed maximum considered earthquake (MCE) response spectra at the fundamental period of each MTCBF (FEMA 2009). Point masses accounting for the seismic weight of the roof and exterior wall cladding were applied at the top of the MTCBF columns. A point mass was not applied to the top of the leaning column. The Hilber, Hughes, Taylor implicit time integrator with α = -0.05 was used to integrate the equations of motion. Again, the Newton-Raphson method was used to solve the nonlinear field equations (Abaqus FEA 2011).

Material behavior for the NLRH analyses was simulated using the nonlinear kinematic/isotropic cyclic hardening model included within Abaqus FEA (2011). Abaqus FEA (2011) simulates the movement and expansion/contraction of the yield surface using exponential functions. To accurately simulate the cyclic stress-strain behavior, the Abaqus FEA (2011) functions must be calibrated using stress-strain data from cyclic tension tests. Cyclic stress-strain data for ASTM A36, ASTM A572, Gr. 50, and ASTM A913 steels, reported by Kauffman and Pense (1999), were used to calibrate the cyclic hardening functions. Based on the data from Kauffman and Pense (1999), the isotropic hardening parameters were similar for all steels tested. The kinematic hardening parameters for ASTM A36 steel, however, were significantly different than those for the ASTM A572, Gr. 50, and ASTM A913 steels. The kinematic hardening parameters calculated from the Kauffman and Pense (1999) data for ASTM A36 steel were used for the ASTM A500, Gr. C, steel in the MTCBF models; and the mean of the kinematic hardening parameters calculated for the ASTM A572, Gr. 50, and ASTM A913 steels were used for the ASTM A992 and ASTM A572, Gr. 50, steels in the MTCBF models. Table 1 summarizes the nonlinear kinematic/isotropic cyclic hardening parameters. It should be noted that two backstresses were used to model the nonlinear kinematic hardening of all materials in the finite element models.

Table 1. Nonlinear kinematic/isotropic hardening model parameters.

	Isotropic		Kinematic			
	Q_∞	b	C_1	γ_1	C_2	γ_2
ASTM A992	6.65	9.89	1147	197	214	0
ASTM A572, Gr. 50	6.65	9.89	1147	197	214	0
ASTM A500, Gr. C	6.65	9.89	430	177	260	0

Geometric Imperfections and Residual Stresses. Geometric imperfections were specified for the in-plane (weak axis) and out-of-plane (strong axis) directions of the columns, and for the out-of-plane direction of the braces. The imperfection geometry was based on eigenvalue buckling analyses of the frames with uniform compressive loads applied at the top of each column. The imperfection magnitudes were based on the AISC *Code of Standard Practice for Steel Buildings and Bridges* (AISC 2010a). In the out-of-plane direction, the column was considered to have a maximum out-of-straightness equal to $H/1000$, where H is the MTCBF height, which is the maximum out-of-straightness permitted between brace points. Similarly, the maximum out-of-straightness for the in-plane direction was $h/1000$ for each panel, where h is the panel height. For the braces, the maximum out-of-straightness was assumed to be $(l/2)/1000$, where l is the distance between the working points at the ends of each brace. The brace half-length was used to calculate the maximum brace out-of-straightness since the tension brace within a panel can provide sufficient lateral stability at the mid-point of the compression brace (Tremblay et al. 2003).

In addition to geometric imperfections, residual stresses were simulated in the columns of the MTCBF finite element models. The Lehigh residual stress pattern (Galambos and Ketter 1958) was used to calculate the magnitudes of the residual normal stresses in the flanges and webs of the columns. To implement the residual

stress pattern in the column flanges, the flanges were partitioned into strips across their width. Appropriate residual stresses were applied to each strip, as well as the column web, using Abaqus FEA (2011) commands. Figure 4 shows the column residual stress pattern and flange discretization. Residual stresses were not simulated in the braces since prior studies indicated that modeling brace residual stresses did not lead to more accuracy in predicted brace buckling response (Izvernari 2007).

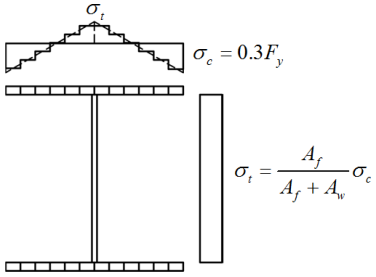

Figure 4. Column residual stress pattern and flange discretization.

STATIC PUSHOVER ANALYSIS

Static pushover (SPO) analysis was conducted to determine the limit states that may be experienced by MTCBFs designed as SCBFs during a large seismic event. Figure 5 shows base shear vs. roof drift ratio data for the scbf-24m-4tier frame. The SPO curve is annotated to show the occurrence of limit states during the analysis. In addition, Figure 6 illustrates the deformed shape of the frame at the points indicated in the SPO curve. In Figure 6, brace buckling is indicated by a filled circle placed on a brace, initial brace yielding is indicated by a dotted line drawn over a brace, and full brace yielding is indicated by a dashed line drawn over a brace.

As shown in Figure 5, the frame response was linear up to Event #1, which was the initiation of brace buckling in all panels. Brace buckling occurred in all panels simultaneously since the buckling strength of the braces in each panel was approximately equal. After Event #1, base shear continued to increase until the ultimate frame capacity was reached at Event #2. This event was defined by the initiation of tension brace yielding within Panel 1. Brace tension yielding initiated within Panel 1 since the yield stress of the braces in this panel was lower than the yield stress of the braces in the remaining panels.

After tension yielding initiated within Panel 1, base shear decreased rapidly until strain hardening of the brace material occurred, which is identified as Event #3. Strain hardening of the brace material, as well as the gusset plate connections at the tier levels, enabled the frame to prevent concentration of inelasticity within Panel 1 by initiating brace tensile yielding in Panel 2. This phenomenon is denoted as Event #4 in Figures 5 and 6. Redistribution of inelastic panel drift was not seen in earlier studies of MTCBFs designed according to the AISC *Seismic Provisions* (2010b) (Imanpour et al. 2013). After Event #4, a small decrease in base shear was noted, but the frame strength remained stable until a roof drift ratio of 0.025 rad was achieved. Numerical convergence was lost at this point, which is denoted Event #5 in Figures 5 and 6. At this point, full yielding of the tension brace in Panel 2 was achieved, as well as initial yielding of the tension brace in Panel 3. Further investigation of the

convergence issue is needed to determine if the stability point of the frame was reached, or if the problem was purely numerical. Nevertheless, the scbf-24m-4tier frame remained stable up to the expected inelastic roof drift $\Delta = 1.5C_d\Delta_e$.

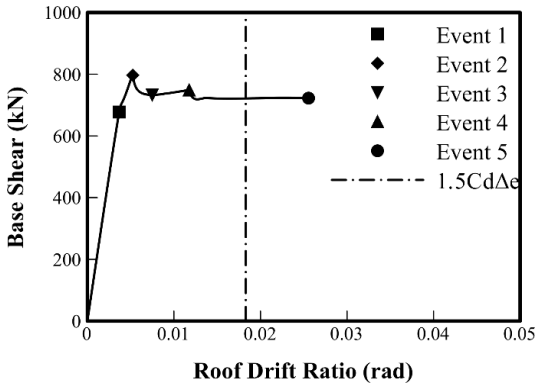

Figure 5. Annotated SPO curve for scbf-24m-4tier frame.

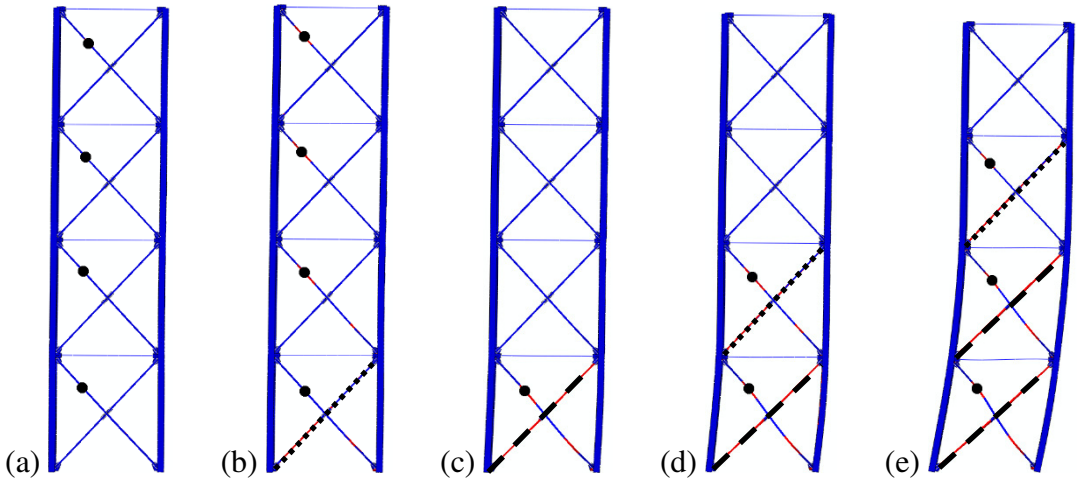

Figure 6. Frame deformed shape: (a) Event 1: Brace buckling; (b) Event 2: Panel 1 initial brace yielding; (c) Event 3: Panel 1 full brace yielding; (d) Event 4: Panel 2 initial brace yielding; (e) Event 5: Panel 2 full brace yielding and Panel 3 initial brace yielding.

The redistribution of inelastic drift was more clearly observed by examining panel drift ratio vs. roof drift ratio data for the scbf-24m-4tier frame, which is illustrated in Figure 7. Initially, inelastic drift concentrated within Panel 1, which is evidenced by the steep slope of the solid black line beginning at a roof drift ratio of 0.005 rad. After achieving a roof drift ratio of 0.012 rad, the scbf-24m-4tier frame was able to distribute inelasticity into Panel 2, which is shown by the steep slope of the dashed line directly below the solid line. Figure 7 indicates, however, that the drift ratio in Panel 1 needed to reach 0.03 rad to initiate redistribution of inelastic drift demand into Panel 2. Therefore, even though the global behavior of the scbf-24m-4tier frame was acceptable according to contemporary seismic provisions (ASCE 2010), the drift ratio within Panel 1 indicated that fracture of the braces in this panel was likely due to excessive inelastic drift (Fell et al. 2009).

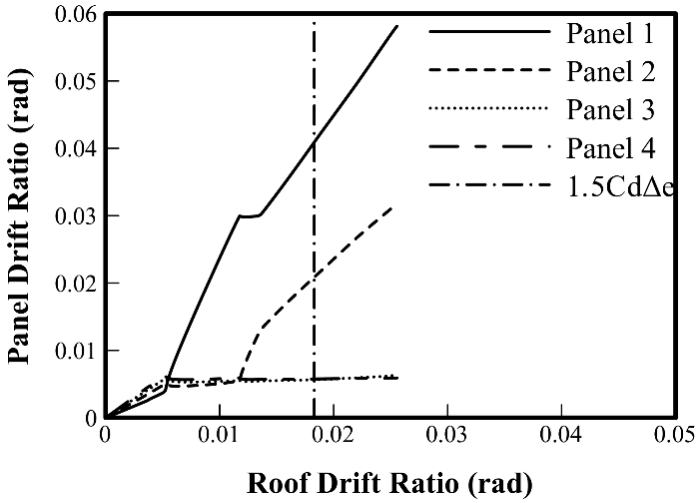

Figure 7. Panel drift ratio vs. roof drift ratio for scbf-24m-4tier frame.

NONLINEAR RESPONSE HISTORY ANALYSIS

To determine the influence of the braced frame connections on the seismic response of MTCBFs subjected to ground acceleration, nonlinear response history analyses of the three-dimensional finite element models were conducted. Imanpour et al. (2013) presented detailed response history results for the scbf-24m-4tier frame under the Imperial Valley, El Centro Array #11, Component #1 ground acceleration record from the FEMA P695 (2009) suite. This ground motion will be denoted GM6. Roof drift ratio vs. time data and panel drift ratio vs. time data for the Abaqus FEA (2011) models are shown in Figures 8 and 9, respectively. The corresponding data from Imanpour et al. (2013), which was obtained using OpenSees (2011) is reproduced in Figure 10.

Figures 8 and 10a indicate that the roof drift ratio vs. time data were similar between Abaqus FEA (2011) and OpenSees (2011). The maximum roof drift ratio achieved, which occurs at approximately 10 sec, was 0.015 rad in the Abaqus FEA (2011) model and 0.018 rad in the OpenSees (2011) model. When comparing Figures 9 and 10b, however, it was found that the maximum drift ratio in Panel 1 was significantly smaller in the Abaqus FEA (2011) model. In the Abaqus FEA (2011) model, the maximum Panel 1 drift ratio was 0.03 rad, while the OpenSees (2011) model predicted a maximum Panel 1 drift ratio of 0.055 rad. The reduction in panel drift is due to the restraint provided at the column tier levels by the strut-column-brace connections.

Although the gusset plate connections reduced the Panel 1 drift ratio in the Abaqus FEA (2011) models, inelastic deformation still concentrated within Panel 1. Therefore, it is likely that the scbf-24m-4tier frame would have experienced ultra-low-cycle fatigue fracture of one, or both, braces within Panel 1. While it is clear that the strut-column-brace connections serve a valuable role in the seismic behavior of MTCBFs, it is expected that they cannot enhance the seismic performance of MTCBFs to acceptable levels without modifications to existing seismic design provisions.

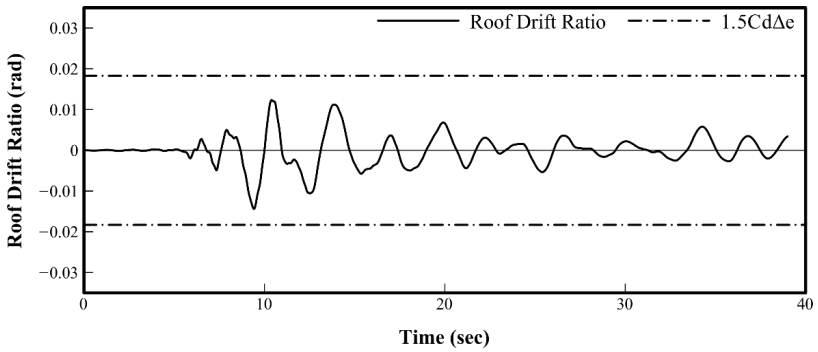

Figure 8. Roof drift ratio vs. time for scbf-24m-4tier-GM6 (Abaqus FEA).

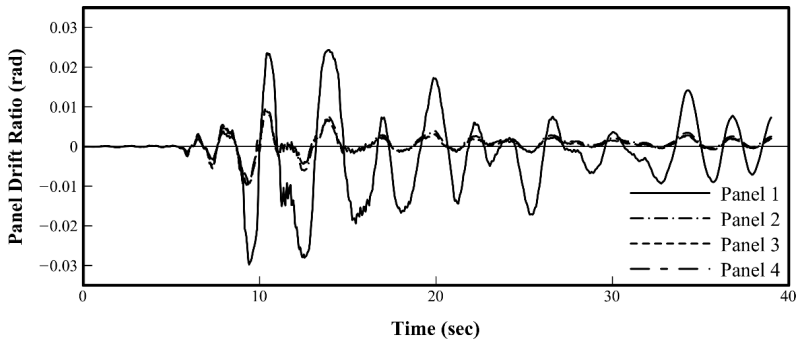

Figure 9. Panel drift ratio vs. time for scbf-24m-4tier -GM6 (Abaqus FEA).

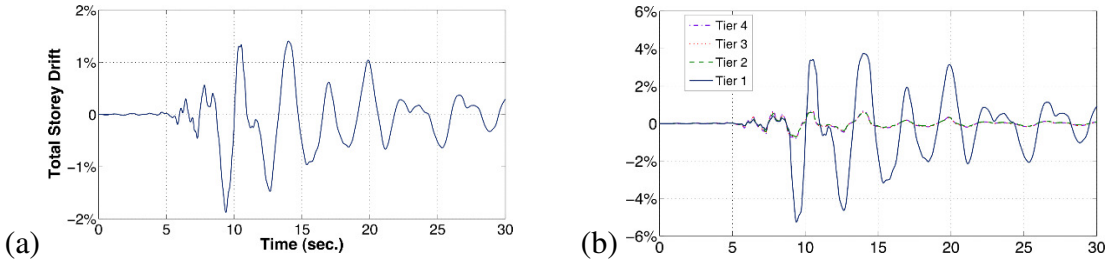

Figure 10. OpenSees (2011) results for scbf-24m-4tier: (a) Total storey drift vs. time; (b) Tier drifts vs. time (Imanpour et al. 2013).

CONCLUSIONS AND FUTURE RESEARCH

In this paper, the results of SPO and NLRH analyses of the seismic behavior of a four-tier CBF designed as an SCBF were presented. The frame behavior was simulated using three-dimensional finite element analysis to accurately model the column axial loading and the interaction of the columns, struts, and braces. The following conclusions were drawn from the results presented herein:

- In-plane flexural restraint provided at the tier levels by strut-column-gusset plate connections increases the ability of columns in MTCBFs to redistribute inelastic drift between panels, which aids in preventing inelastic drift concentrations.
- In addition, the strut-column-gusset plate connections may significantly reduce the panel drift ratios achieved in MTCBFs during large seismic events.

- In the scbf-24m-4tier frame examined, however, panel drifts were observed during SPO and NLRH analyses that indicated the potential for ultra low cycle fatigue fracture of the braces.
- Future investigations of the seismic behavior of MTCBFs will focus on the 9m-2tier and 15m-3tier frames mentioned above. In addition, the need for torsional restraint at the tier levels will be reexamined in light of the fact that torsional deformation due to brace buckling was not observed during the present study.
- Finally, the results of computational simulations of the seismic behavior of MTCBFs need to be verified with large scale experiments.

Funding for this research was provided by the American Institute of Steel Construction. The computational simulations described herein were partially conducted using the Extreme Science and Engineering Discovery Environment, which is supported by National Science Foundation grant number OCI-1053575. The opinions, findings, and conclusions in this paper are those of the authors and do not necessarily reflect those acknowledged here.

REFERENCES

Abaqus FEA (Version 6.11-1) [software] (2011). Dassault Systemes, www.3ds.com.

American Society of Civil Engineers (ASCE) (2010). *Minimum Design Loads for Buildings and Other Structures*. ASCE 7-10, ASCE, Reston, Virginia.

American Institute of Steel Construction (AISC) (2010a). *Code of Standard Practice for Steel Buildings and Bridges*. AISC 303-10, AISC, Chicago, Illinois.

American Institute of Steel Construction (AISC) (2010b). *Seismic Provisions for Structural Steel Buildings*. ANSI/AISC 341-10, AISC, Chicago, Illinois.

American Institute of Steel Construction (AISC) (2010c). *Specification for Structural Steel Buildings*. ANSI/AISC 360-10, AISC, Chicago, Illinois.

Federal Emergency Management Agency (FEMA) (2009). *Quantification of Building Seismic Performance Factors*. FEMA P695, prepared by the Applied Technology Council, Washington, D.C.

Fell, B. V., Kanvinde, A. M., Deierlein, G. G., and Myers, A. T. (2009). "Experimental investigation of inelastic cyclic buckling and fracture of steel braces." *Journal of Structural Engineering*, ASCE, 135(1), 19-32.

Galambos, T. V. and Ketter, R. L. (1958). *Columns under Combined Bending and Thrust*. Fritz Engineering Laboratory Report 205A.21, Lehigh University, Bethlehem, Pennsylvania.

Gross, J. and Cheok, G. (1988). *Experimental Study of Gusseted Connections for Laterally Braced Steel Buildings*. National Institute of Science and Technology, Gaithersburg, Maryland.

Helwig, T. A. and Yura, J. A. (1999). "Torsional bracing of columns." *Journal of Structural Engineering*, ASCE, 125(5), 547-555.

Imanpour, A., Stoakes, C., Tremblay, R., Fahnestock, L., and Davaran, A. (2013). "Seismic stability response of columns in multi-tiered braced steel frames for industrial applications." *Proceedings, Structures Congress 2013*, ASCE, Pittsburgh, Pennsylvania, May 2-4.

Imanpour, A., Tremblay, R., and Davaran, A. (2012a). "Seismic evaluation of multi-panel steel concentrically braced frames." *Proceedings, 15th World Conference on Earthquake Engineering*, Lisbon, Portugal, Paper No. 2996.

Imanpour, A., Tremblay, R., and Davaran, A. (2012b). "Seismic performance of steel concentrically braced frames with bracing members intersecting columns between floors." *Proceedings, Behavior of Steel Structures in Seismic Areas (STESSA 2012)*, Santiago, Chile, January 9-11.

Imanpour, A. and Tremblay, R. (2012). "Analytical assessment of stability of unbraced column in two-panel concentrically braced frames." *Proceedings, 3rd International Structural Specialty Conference (CSCE 2012)*, Edmonton, Alberta, Canada, Paper No. STR-1218.

Izvernari, C. (2007). The Seismic Behavior of Steel Braces with Large Sections, Doctoral Dissertation, Department of Civil, Geological, and Mining Engineering, Ecole Polytechnique, Montreal, Quebec, Canada.

Kauffman, E. J. and Pense, A. W. (1999). *Characterization of Cyclic Inelastic Strain Behavior on Properties of A572 Gr. 50 and A913 Rolled Sections*, AISC-PITA Project Progress Report, ATLSS Research Center, Lehigh University, Bethlehem, Pennsylvania.

OpenSees (Version 2.2.2) [software] (2011). Pacific Earthquake Engineering Research Center, University of California, Berkeley, California, opensees.berkeley.edu.

Peng, S. W. (2001). *Seismic Resistant Connections for Concrete Filled Tube Columns-to-WF Beam Moment Resisting Frames*, Doctoral Dissertation, Department of Civil and Environmental Engineering, Lehigh University, Bethlehem, Pennsylvania.

Richard, J. M. (1986). "Analysis of large bracing connection designs for heavy construction." *Proceedings, 1986 National Engineering Conference*, AISC, June.

Roufegarinejad, A. and Tremblay, R. (2012). "Finite element modeling of the inelastic cyclic response and fracture life of square tubular steel bracing members subjected to seismic inelastic loading." *Proceedings, Behavior of Steel Structures in Seismic Areas*, Santiago, Chile, January 9-11.

Stoakes, C. D. and Fahnestock, L. A. (2012a). "Cyclic flexural analysis and behavior of beam-column connections with gusset plates." *Journal of Constructional Steel Research*, Elsevier, 72(2012), 227-239.

Stoakes, C. D. and Fahnestock, L. A. (2012b). "Influence of weak-axis flexural yielding on the strong-axis buckling strength of wide flange columns." *Proceedings, 2012 Annual Stability Conference*, SSRC, Grapevine, Texas, April 18-21.

Stoakes, C. D. and Fahnestock, L. A. (2011). "Cyclic flexural testing of concentrically braced frame beam-column connections." *Journal of Structural Engineering*, ASCE, 137(7), 739-747.

Thorton, W. A. (1991). "On the analysis and design of bracing connections." *Proceedings, 1991 National Engineering Conference*, AISC, June.